Bioresource Technology Reports 33 (2026) 102597

Contents lists available at ScienceDirect

Bioresource Technology Reports

journal homepage: www.sciencedirect.com/journal/bioresource-technology-reports

# Enhancing the interpretation of biochemical methane potential assays through methane production kinetics: A case study with grass clippings and fruit-vegetable waste

Brahim Arhoun [a,1], Belén Muñoz-Cabello [b,1], Souad Benaisa [a], Cesar Gomez-Lahoz [b], Carlos Vereda-Alonso [b,*], María del Mar Cerrillo-González [b]

[a] Laboratory of Water, Studies and Environmental Analysis, Faculty of Sciences, Abdelmalek Essaadi University, Tetouan, Morocco
[b] Chemical Engineering Department, Faculty of Sciences, University of Malaga, 29071, Malaga, Spain

ARTICLE INFO

*Keywords:*
Urban biomass
Grass clippings
Fruit and vegetable waste
Biochemical methane potential
Size reduction
Mixture ratio
Kinetic modeling

ABSTRACT

Anaerobic co-digestion (AcoD) of grass waste (GS) with fruit and vegetable waste (FVW) was evaluated to improve methane generation from lignocellulosic biomass. Batch BMP tests were performed using raw grass (GSr), size-reduced grass (GSp), and GS:FVW mixtures.

FVW exhibited high biodegradability (453 Nml $CH_4$/gVS; BDI 97.7%), whereas GS showed markedly lower conversion (169 Nml $CH_4$/gVS; BDI 41.2%). Particle-size reduction of grass from 20 mm to <5 mm increased the methane production rate but did not significantly affect ultimate methane yield. Co-digestion behavior was strictly additive, with CPI values approximately equal to 1 for all mixtures. Among the kinetic formulations, the Two-fractions First-order and Multi-stages models provided the best description of methane production, particularly when BMP values were fixed to their theoretical predictions derived from CHNSO. A mathematical demonstration showed that the analytic expression of the Multi-stage model can be transformed into the Two-fractions First-order formulation, confirming their mathematical equivalence despite differing conceptual interpretations.

These results highlight the suitability of FVW as a co-substrate for GS digestion and demonstrate the value of kinetic modeling for interpreting and predicting biomethane production from slowly degradable feedstocks.

## 1. Introduction

Rising global food and energy demand, together with geopolitical pressures, increases energy costs and complicates carbon-neutrality efforts (Jiang et al., 2021; Phuttaro et al., 2023), while growing GHG emissions and organic-waste accumulation intensify environmental challenges. (Offermanns et al., 2023; Yasim and Buyong, 2023). Anaerobic digestion (AD) offers a practical solution by stabilizing organic residues while generating biogas and producing nutrient-rich digestate suitable for agricultural reuse.(Edwiges et al., 2019; Egwu et al., 2022; Seppälä et al., 2009). Owing to its operational simplicity, flexibility in feedstock selection, and positive environmental impact, AD is increasingly integrated into circular-economy strategies and municipal waste-management systems.

Urban grass clippings and maintenance-derived grass waste represent a widely available lignocellulosic biomass stream that does not compete with food production (Massanet-Nicolau et al., 2015; Melts et al., 2014). Reported grass yields vary widely with management and climate, but typical productive swards deliver on the order of 10–18 t dry matter (DM) $ha^{-1}$ $yr^{-1}$, while low-intensity or roadside grasslands may yield only a few t DM $ha^{-1}$ $yr^{-1}$ (Dickeduisberg et al., 2017; Meyer et al., 2014; Phuttaro et al., 2023). However, the biodegradability of grass is restricted by its structural composition, characterized by high cellulose and hemicellulose content and a relatively rigid lignin fraction (Edwiges et al., 2019). Reported specific methane yields (SMY) of grass typically range from 188 to 311 mL $CH_4$ $g^{-1}$ VS, varying with species, harvest time, and growth stage (Butkutė et al., 2014; Melts et al., 2014; Prochnow et al., 2009; Seppälä et al., 2009; Song et al., 2023). In addition, grass frequently exhibits a high C/N ratio (approximately 25–55) (Nuchdang et al., 2015; Phuttaro et al., 2023), which can limit

* Corresponding author.
*E-mail address:* cvereda@uma.es (C. Vereda-Alonso).
[1] Equal contribution.

https://doi.org/10.1016/j.biteb.2026.102597
Received 20 October 2025; Received in revised form 7 January 2026; Accepted 23 January 2026
Available online 29 January 2026

microbial activity and reduce process stability when digested alone.

Fruit and vegetable waste (FVW) generation at wholesale markets typically ranges from a few to several tens of tonnes per day, with regional wholesale networks reaching around 100–200 t $day^{-1}$ (Mokjatturas et al., 2025; Trujillo-Reyes et al., 2023). FVW, in contrast, is rich in readily degradable carbohydrates, and micronutrients. High moisture content and elevated volatile solids fractions make FVW an efficient co-substrate for stabilizing the digestion of carbon-rich biomasses such as grass (D' Silva et al., 2022). SMY values for FVW are typically higher, often exceeding 320 mL $CH_4$ $g^{-1}$ VS, depending on composition and season (Arhoun et al., 2019; Edwiges et al., 2018). These complementary characteristics indicate a strong potential for co-digestion to balance nutrients, dilute inhibitors, and promote synergistic degradation pathways.

Anaerobic co-digestion (AcoD) provides numerous ecological, technological, and economic benefits by improving digester stability and performance. Advantages include inhibitor dilution, balanced nutrient availability, and optimized C/N ratio, all of which contribute to enhanced microbial activity and substrate degradation (D' Silva et al., 2022; Kouas et al., 2018). AcoD strategies maximize biogas production and maintain process stability, particularly when co-digesting grass with substrates such as animal manure, sewage sludge, microalgae, food waste and the organic fraction of municipal solid waste, yielding SMYs ranging from 100 to 400 mL $CH_4$ $g^{-1}$ VS (Song et al., 2023). The mixing ratio of substrates is a critical parameter influencing degradability and biogas yield.

Pretreatment strategies, particularly mechanical size reduction, are frequently applied to improve accessibility of lignocellulosic biomass (Phuttaro et al., 2023; Sunar et al., 2025). Reducing particle size increases the surface area available for hydrolysis and can shorten the lag phase (Jomnonkhaow et al., 2021). Methane production rate generally increases with decreasing particle size, but further reduction beyond a certain threshold does not enhance SMY. Particle size should therefore be reduced only until SMY plateaus (0.250–0.380 mm for *Hybrid Pennisetum* and $< 1$ cm for grass silage) (Kang et al., 2019; Wall et al., 2015).

Despite the significant availability of grass waste and FVW, studies systematically evaluating the combined effect of co-digestion ratio and grass particle size remain limited. Most works focus either on pretreatment or on substrate mixture optimization, but not on their interaction (Hmeekong et al., 2025; Warade et al., 2025). Batch Biochemical Methane Potential (BMP) assays are widely used to assess the anaerobic biodegradability of various organic wastes. BMP tests also serve as benchmarks for comparing substrate biodegradability and evaluating the impact of pretreatment methods on methane yield (Aguilar-Aguilar et al., 2025; Almeida et al., 2021; El Gnaoui et al., 2022).

Recent studies (Alrefaey et al., 2024; Scherzinger et al., 2022; Weber et al., 2026) have calculated the parameters of kinetic models from the substrate composition, providing a rapid means to estimate BMP. Nevertheless, discrepancies between experimental and theoretical BMP values highlight the need for kinetic modeling to better interpret degradation dynamics. Furthermore, the most suitable kinetic model is largely determined by the type of substrate involved (Karki et al., 2022).

This study is structured into three primary parts. First, batch BMP experiments were conducted to investigate the effects of varying mixing ratios of grass and fruit and vegetable waste (FVW) on methane yield, including the impact of grass particle size reduction in co-digestion with FVW. Second, theoretical BMP values were calculated based on elemental composition to estimate the effects of co-digestion and pretreatment on substrate biodegradability. Finally, six kinetic models were applied to characterize the degradation kinetics of the studied substrates. These included the First-order, two-fraction First-order, Monod-type, Modified Gompertz, Superimposed, and Multi-stage models.

By integrating experimental BMP data with kinetic modeling, a more comprehensive understanding of anaerobic biodegradability can be achieved. This synergy not only enhances the interpretation of experimental results but also improves the predictive accuracy of biogas potential, ultimately supporting more effective optimization of AD processes.

## 2. Materials and methods

### 2.1. Inoculum and substrates

FVW was sourced from the rejects produced at Mercamálaga, the main wholesale market of Málaga (Spain). This market generates approximately ten metric tons of FVW daily. A 20 kg sample of FVW, representative of the wholesale market's production, was collected, with a detailed composition provided in Table 1-S (supplementary material). The FVW was manually chopped in the laboratory and then ground using a blender. The processed material was stored in 200 mL bottles at −20 °C until use.

Grass (*Cynodon dactylon*) (GS) was collected from a garden at the University of Malaga, Spain. After harvesting, the fresh grass was cut into 20 mm lengths using a chopper machine. The raw grass (GSr) was then ground with a coffee mill and sieved to a particle size of less than 5 mm to enhance the contact between the biomass and inoculum. Both the raw and treated grass (GSp) were placed in 200 mL plastic vials and stored in a refrigerator at −20 °C until use. The grass samples were used in the experiment without drying.

The inoculum is a crucial component in the BMP test, providing the necessary microorganisms for AD. This study used digested sludge as the inoculum, sourced from a mesophilic anaerobic digester operating at 35 ± 1 °C with a hydraulic retention time (HRT) of 20 days, located in Málaga, Spain. The digested sludge was transported from the wastewater treatment plant (WWTP) to the laboratory, where it was maintained under the same conditions without any feed for 72 h to lower its biogas production before starting the BMP assays. The key characteristics of the inoculum and those of the FVW and GS are detailed in Section 3 "Results and discussion", Table 2.

### 2.2. BMP experimental tests

Glass bottles with a capacity of 500 mL were used as anaerobic reactors, each with a working volume of 400 mL. The mixing ratios of GSr and GSp to FVW were varied on a wet weight basis at 100:0, 80:20, 60:40, 40:60, 20:80, and 0:100. The corresponding ratios in terms of volatile solids (VS) and total solids (TS) for these wet weight mixtures are detailed in Table 1, along with the total substrate VS concentration and TS content resulted from each mixing ratio.

Three blank bottles containing only inoculum were included as controls to account for methane generation solely from the inoculum. The VS ratio of inoculum to substrate in all bottle reactors was 4:1. This high inoculum ratio is used to prevent the accumulation of volatile fatty acids and to avoid bacterial inhibition under acidic conditions. The BMP

**Table 1**
Wet weight mixing ratios and corresponding TS and VS fractions of substrate mixtures GS:FVW.

| | | | | | | |
|---|---|---|---|---|---|---|
| Total mass | 100:0 | 80:20 | 60:40 | 40:60 | 20:80 | 0:100 |
| Total solids | 100:0 | 96.1:3.9 | 90.3:9.7 | 80.6:19.4 | 60.9:39.1 | 0:100 |
| Volatile solids | 100:0 | 95.8:4.2 | 89.4:10.6 | 79.0:21.0 | 58.5:41.5 | 0:100 |
| Total substrate (VS) concentration (%) | 0.71 | 0.75 | 0.76 | 0.77 | 0.77 | 0.77 |
| TS concentration (%) | 5.3 | 5.6 | 5.7 | 5.8 | 5.8 | 5.8 |

procedures were adapted from (Phuttaro et al., 2023), and the experiment was conducted without supplementing additional nutrients or trace elements. The schematic of the BMP experimental setup is shown in Fig. 1.

The bottle reactors were loaded with a mixture of the substrate, and immediately afterward, oxygen was purged by flushing the bottles with a $N_2$ stream for approximately 2 min, and then the required amount of inoculum was added while the $N_2$ stream was maintained. Immediately after the $N_2$ stream was stopped, the bottles were sealed with rubber stoppers and gas collection tubing was connected. The bottles were then placed in a shaker, with the temperature maintained at 35 ± 1 °C and stirring set at 50 rpm. Specific methane production was corrected for the gas volume produced by the inoculum without substrate, normalized to standard conditions (dry gas at 273.15 K and 1013.25 mbar) and reported per gram of VS added (mL $g_{VS}^{-1}$).

### 2.3. Analytical methods

The substrates and inoculum initial samples underwent triplicate analysis, with an additional sample of the digestate on the final day of the experiment. Parameters such as TS, VS, and pH were obtained according to standardized methods outlined by APHA (1998). Hemicellulose, cellulose, and lignin were determined as described in (Mansor et al., 2019). Elemental analysis for carbon (C), hydrogen (H), nitrogen (N), sulfur (S), and oxygen (O) content was conducted using a Perkin Elmer CHNSO 2400 apparatus.

The biogas production was measured every day by a volume displacement method; the composition of biogas was determined daily by gas chromatography (Perkin-Elmer Autosystem) with a thermal conductivity detector and a Supelco column (15 ft. × 1/8″; 60/80 carboxy 1000). The oven, injector, and detector temperatures were 180 °C, 180 °C and 220 °C, respectively. Helium was used as carrier gas at a 30 mL/min flow rate.

### 2.4. BMP theoretical model and calculation

#### 2.4.1. Stoichiometry analysis and biodegradability index

Theoretical biochemical methane potential ($BMP_{theo}$) was determined using a modified Buswell and Mueller's equation, incorporating nitrogen and sulfur as described by (Phuttaro et al., 2023). This calculation was based on the elemental composition of the substrate (C, H, O, N, and S), where the percentages of these elements were applied in a stoichiometric equation to estimate the methane yield (Rodrigues et al., 2019).

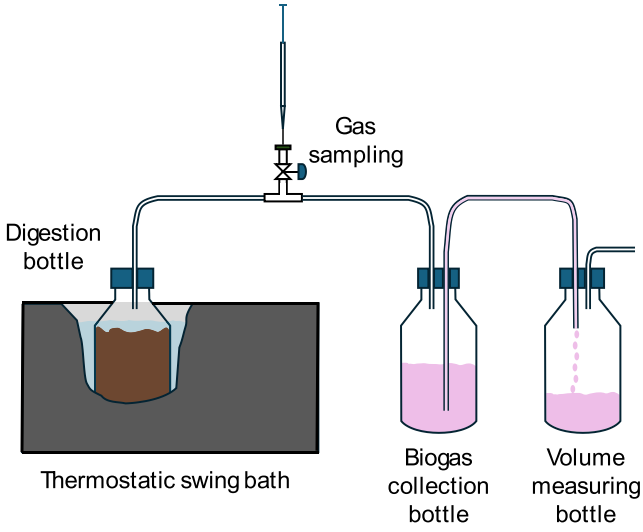


**Fig. 1.** Schematic of the BMP experimental setup.

Biodegradability index (*BDI*) percentage was calculated after the following equation (Nielfa et al., 2015; Yasim and Buyong, 2023).

$$BDI = \frac{BMP_{exp}}{BMP_{theo}} \times 100 \quad (2)$$

where $BMP_{exp}$ (mL $CH_4$ $g_{VS}^{-1}$) and $BMP_{theo}$ (mL $CH_4$ $g_{VS}^{-1}$) represented methane generation obtained from the experimental setup and theoretical calculated respectively.

$$C_aH_bO_cN_dS_e + \left(a - \frac{b}{4} - \frac{c}{2} + \frac{3d}{4} + \frac{e}{2}\right)H_2O \rightarrow \left(\frac{a}{2} + \frac{b}{8} - \frac{c}{4} - \frac{3d}{8} - \frac{e}{4}\right)CH_4 + \left(\frac{a}{2} - \frac{b}{8} + \frac{c}{4} + \frac{3d}{8} + \frac{e}{4}\right)CO_2 + d\,NH_3 + e\,H_2S$$

$$BMP_{theo} = \frac{22\,400 \times \left(\frac{a}{2} + \frac{b}{8} - \frac{c}{4} - \frac{3d}{8} - \frac{e}{4}\right)}{12a + b + 16c + 14d + 32e} \quad (1)$$

Where *a*, *b*, *c*, *d*, and *e* represent the number of moles of C, H, O, N, and S, respectively that are present in each 100 g of dry sample, as obtained in the elemental analysis. The 22,400 factor corresponds to the molar volume (mL $mol^{-1}$) at standard conditions (dry gas at 273.15 K and 1013.25 mbar). Thus, $BMP_{theo}$ is expressed in units of mL $CH_4$ per gram of VS (mL $CH_4$ $g_{VS}^{-1}$).

#### 2.4.2. Volatile solids reduction

The removal of volatile solids ($VS_{removal}$) was calculated using the method described by Di Maria et al. (2015):

$$VS_{removal} = \frac{VS_{t=0} - VS_{t=end}}{VS_{t=0}} \times 100 \quad (3)$$

where $VS_{t=0}$ is the volatile solids content at the start, and $VS_{t=end}$ is the content at the end of the experiment.

#### 2.4.3. Co-digestion performance index

Higher methane yields are expected in anaerobic co-digestion due to the combined organic content and potential synergistic effects of mixed substrates. These effects, including the dilution of inhibitory by-products and enhanced microbial metabolism, improve biodegradability. To assess synergy, the BMP of AcoD is compared with the weighted sum of individual substrates using the co-digestion performance index (*CPI*) (Ebner et al., 2016; Edwiges et al., 2018; Phuttaro et al., 2023).

$$CPI = \frac{BMP_{mix\ G:F}}{(G \times BMP_G) + (F \times BMP_F)} \tag{4}$$

Where $G$ and $F$ are the VS fraction of grass and FVW in the mixture ($0 < G,F < 1$), $BMP_{mix\ G:F}$ (mL $g_{VS}^{-1}$) is the cumulative methane yield of the mixture of substrates at ratio G:F, $BMP_G$ (mL $g_{VS}^{-1}$), and $BMP_F$ (mL $g_{VS}^{-1}$) are the cumulative methane yield of grass and FVW respectively.

### 2.5. Kinetic models

Six kinetic models were studied, incorporating both mathematical and biological parameters, to assess the impact of pretreatment and co-digestion at different mixture ratios on digestion kinetics. The models used were the First-Order Kinetic Model, the Two-Fraction First-Order Kinetic Model, the Monod type Model, the Modified Gompertz Model, the Superimposed Model, and Multi-stage Model. These models were employed to evaluate the predicted methane potential of the substrates. In all models, $V_{CH_4}$ represents the predicted volume of methane produced at time $t$ per unit mass of volatile solids $\left(mL_{CH_4}\ g_{VS}^{-1}\right)$, and $BMP$ denotes the maximum methane yield per unit mass of VS, which is the biomethane potential.

#### 2.5.1. First-order kinetic model (FO)

The FO model is a simple approach, but it does not account for conditions that optimize biological activity or indicate potential system failures. In AD, hydrolysis is typically seen as the rate-limiting step (Kafle and Chen, 2016). FO model requires two parameters to estimate the predicted methane potential (Edwiges et al., 2019; Nielfa et al., 2015).

$$V_{CH_4} = BMP\ (1 - \exp(-k_1 t)) \tag{5}$$

Where $k_1$ ($d^{-1}$) is the apparent hydrolysis rate coefficient and $t$ (d) is the digestion time.

#### 2.5.2. Two fractions first-order kinetic model (TFFO)

This is also known as two-phase (multi-phase) exponential model, in which the total methane-production curve results from the additive contribution of two kinetic components that operate as parallel degradation processes, each describing the conversion of a distinct substrate fraction (López et al., 2011). The TFFO assumes two biodegradable fractions with independent first-order degradation rates: rapid and slow (García-Gen et al., 2015).

$$\begin{aligned} V_{CH_4} &= BMP\ (1 - \alpha\exp(-k_f t) - (1-\alpha)\exp(-k_s t)) \\ &= BMP_f\left[1 - \exp(k_f t)\right] + BMP_s[1 - \exp(-k_s t)] \end{aligned} \tag{6}$$

Where α represents the share of rapidly degradable substrates components, $k_f$ ($d^{-1}$) and $k_s$ ($d^{-1}$) are the first order reaction constants for the fast and slow degradable fraction, respectively, and $BMP_f$ and $BMP_s$ are the BMP of the rapid and slow phases, respectively.

#### 2.5.3. Monod type kinetic model (MT)

The MT model is widely used in BMP testing to describe microbial growth and substrate utilization during AD.

$$V_{CH_4} = BMP\left(\frac{kt}{1+kt}\right) \tag{7}$$

Where $k$ ($d^{-1}$) is the rate constant.

#### 2.5.4. Modified Gompertz model (MG)

The key parameters of the MG model are the maximum biomethane production potential, the maximum daily production rate, and the lag phase. The lag phase is a critical indicator of AD efficiency, representing the minimum time required for microbial acclimation before the onset of biogas production. It reflects the relationship between methane generation and microbial activity (Kafle and Chen, 2016).

$$V_{CH_4} = BMP\exp\left(-\exp\left(\frac{R_m \exp(1)}{BMP}(\lambda - t) + 1\right)\right) \tag{8}$$

Where $R_m$ is the maximal methane production rate (mL $g_{VS}^{-1}d^{-1}$) and $\lambda$ (d) is the lag phase time.

#### 2.5.5. Superimposed model (S)

The S model combines the MG and FO kinetic formulations to represent biogas production driven by two distinct degradable fractions. It assumes that readily biodegradable compounds generate an initial rapid methane production peak, while more recalcitrant substrates degrade slowly and contribute to a second peak (Karki et al., 2022).

$$V_{CH_4} = BMP_1\ (1 - \exp(-kt)) + BMP_2\exp\left(-\exp\left(\frac{R_m \exp(1)}{BMP_2}(\lambda - t) + 1\right)\right) \tag{9}$$

Where $BMP_1$ and $BMP_2$ are the BMPs from the easily and poorly biodegradable substrates, respectively $\left(mL_{CH_4}\ g_{VS}^{-1}\right)$, and $k$ ($d^{-1}$) is the methane production rate constant.

#### 2.5.6. Multi-stage model (MS)

The MS model represents anaerobic digestion as a sequence of mechanistically linked stages operating as serial degradation processes, where the output of one stage directly influences the next. In contrast to multi-phase approaches that simply sum the contribution of separate phases, the MS formulation explicitly accounts for the dynamic interactions between stages, such as hydrolysis of complex substrates followed by fermentation of the released soluble intermediates.(Karki et al., 2022; López et al., 2011).

$$V_{CH_4} = BMP_S\ (1 - \exp(-k_1 t)) + BMP_I\ (1 - \exp(-k_2 t)) + BMP_{IS}\left[1 - \frac{k_2 \exp(-k_1 t)}{k_2 - k_1} - \frac{k_1 \exp(-k_2 t)}{k_1 - k_2}\right] \tag{10}$$

Where $BMP_S$ and $BMP_I$ are the BMP in each stage: substrate and intermediate $\left(mL_{CH_4}\ g_{VS}^{-1}\right)$, $BMP_{IS}$ is the BMP corresponding to their interactions $\left(mL_{CH_4}\ g_{VS}^{-1}\right)$, and $k_1$ ($d^{-1}$) and $k_2$ ($d^{-1}$) are the methane production rate constant in each stage.

#### 2.5.7. Model selection and performance evaluation

The values of the parameters of the kinetic models were determined through nonlinear regression analysis using the Microsoft Excel Solver. This regression was made by minimizing the root mean square error

(RMSE) defined as follows:

$$RMSE = \sqrt{\frac{\sum_{i=1}^{n}\left(V_{CH_4}^{exp} - V_{CH_4}^{model}\right)^2}{n-1}} \quad (11)$$

where $V_{CH_4}^{exp}$ (mL $g_{VS}^{-1}$) and $V_{CH_4}^{model}$ (mL $g_{VS}^{-1}$) represent the experimental and model-predicted volumes of methane released for each time value, and $n$ is the number of data points.

The Akaike Information Criterion (AIC) is used to compare statistical models by measuring their goodness of fit while penalizing model complexity. In this case, the general formula for AIC when using the least squares model fitting is (Burnham and Anderson, 2004):

$$AIC = 2\,k + n\ln\left(\frac{\sum_{i=1}^{n}\left(V_{CH_4}^{exp} - V_{CH_4}^{model}\right)^2}{n}\right) \quad (12)$$

Where $k$ is the number of estimated parameters in the model and $n$ is the number of experimental observations.

AIC only assesses the relative quality of a model compared to alternative models. The model with the lowest AIC value is considered the best-performing, as a lower AIC indicates a better balance between goodness of fit and model simplicity.

Once AIC has identified the best model among the six candidates, it is essential to further evaluate its predictive performance and goodness of fit. The RMSE and the coefficient of determination ($R^2$) provide complementary insights:

$$R^2 = 1 - \frac{\sum_{i=1}^{n}\left(V_{CH_4}^{exp} - V_{CH_4}^{model}\right)^2}{\sum_{i=1}^{n}\left(V_{CH_4}^{exp} - \overline{V_{CH_4}^{exp}}\right)^2} \quad (13)$$

Where $\overline{V_{CH_4}^{exp}}$ (mL $g_{VS}^{-1}$) is the mean value of all the experimental volumes obtained during the experiment.

A lower RMSE value indicates a better fit, while $R^2$ should be close to 1 to demonstrate a strong correlation between observed and predicted values.

#### 2.5.8. Statistical analysis

The BMP data were statistically analyzed using the Analysis ToolPak add-in of Microsoft Excel (Microsoft Office 365). A two-way ANOVA was performed to assess the effects of grass type (GSr vs. GSp) and GS:FVW ratio on BMP.

## 3. Results and discussion

The results are presented as follows: First, the compositions of inoculum, FVW, and GS were analyzed. Next, the experimental and theoretical BMP values were determined for FVW, GSr, GSp, and their mixtures with FVW at different proportions. Finally, the six kinetic models were applied, and the best-fitting model was identified based on their performance.

### 3.1. Inoculum and substrates characterization

The samples were analyzed in triplicate to determine the composition of the inoculum and substrates, with the results summarized in Table 2.

The analysis reveals that GS has a higher TS and VS than FVW. Specifically, the VS content, expressed as a percentage of TS, was 64% for the inoculum, 88% for FVW, and 79% for GS, indicating a high organic matter content in both substrates, which is favorable for AD. The hemicellulose, cellulose, and lignin contents in GS were significantly higher than those in FVW, suggesting that FVW is more biodegradable than GS.

**Table 2**
Characteristics of the substrates.

| Parameters | Inoculum | FVW | GS |
|---|---|---|---|
| pH | 7.1 | 5.1 | – |
| Total solid (%) | 4.95 ± 0.02 | 8.50 ± 0.13 | 53.0 ± 1.3 |
| Volatile solid (%) | 3.16 ± 0.02 | 7.45 ± 0.05 | 41.9 ± 1.0 |
| VS/TS | 0.64 | 0.88 | 0.79 |
| C (%) | 30.7 ± 1.3 | 46.8 ± 0.6 | 34.5 ± 0.3 |
| H (%) | 4.54 ± 0.20 | 6.03 ± 0.08 | 4.44 ± 0.13 |
| N (%) | 5.13 ± 0.20 | 2.28 ± 0.08 | 1.46 ± 0.13 |
| O (%) | 24.0 ± 0.6 | 41.2 ± 0.6 | 36 ± 3 |
| S (%) | 1.64 ± 0.16 | 0.134 ± 0.008 | 0.161 ± 0.019 |
| (C + H + N + O + S) (%) | 66.1 | 96.4 | 76.3 |
| C/N | 6.00 | 20.54 | 23.66 |
| Hemicellulose (%) | | 5.8 ± 0.7 | 67.8 ± 0.6 |
| Cellulose (%) | | 2.0 ± 1.7 | 13.7 ± 1.5 |
| Lignin (%) | | 0.14 ± 0.04 | 9.9 ± 0.8 |
| Extractable (%) | | 92.1 ± 1.1 | 8.57 ± 0.10 |

The pH values of the substrates varied, ranging from neutral in the inoculum to acidic in FVW. Elemental composition analysis, referred to TS, revealed that FVW has a higher carbon content than GS. The carbon-to-nitrogen (C/N) ratio was lower in the inoculum. At the same time, it ranged between 20 and 24 in FVW and GS, aligning with the nutrient balance required for optimal bacterial growth during AD (El Gnaoui et al., 2022; Phuttaro et al., 2023; Rangseesuriyachai et al., 2023). This indicates that if any synergism is observed in their co-digestion, it would be unlikely to result from improved nutrient balance. It can be observed that the sum of the five elements reported yields a value close to the VS/TS ratio, as could be expected, indicating that these elements are the main part of the VS.

From these values, it is clear that grass residues present a moisture content too high for energy recovery through thermal processes, but this value may be too low for the recovery by AD. Therefore, co-digestion with substrates with higher moisture content could be an optimal strategy for enhancing energy recovery while minimizing resource consumption. This study aims to investigate this approach further.

### 3.2. Experimental BMP and effect of pre-treatment

The cumulative methane generation for FVW, GSr, and GSp is shown in Fig. 2, with results recorded over 33 days of digestion. FVW demonstrated a BMP of 453 ± 16Nml $CH_4/g_{VS}$ and a biodegradability of 97.7%, as detailed in Table 3. For instance, Edwiges et al. (2018) conducted a year-long evaluation of FVW, reporting BMP values ranging from 288 to 516 Nml $CH_4/g_{VS}$, highlighting FVW's susceptibility to seasonal variations in composition, which can significantly influence BMP.

For GSr and GSp, BMP values were 163 ± 4 and 175 ± 5 Nml $CH_4/g_{VS}$, respectively. These values are lower than those reported in other studies, (Edwiges et al., 2019; Nolan et al., 2016), which found BMP values of 264 and 285 Nml $CH_4/g_{VS}$. As expected, the application of pretreatment did not lead to a significant increase in BMP. Two-way ANOVA confirmed that the BMP values were significantly affected by the GS:FVW mixing ratio for both GSr and GSp co-digestions ($p < 0.001$). However, particle-size reduction of grass did not result in a statistically significant change in BMP in any of the mixtures.

FVW achieved the highest methane production rate from the first day of the BMP test, with a peak of 147 Nml $CH_4/g_{VS}$/day, indicating its higher biodegradability. In contrast, GSr reached its maximum daily production on the third day with 15 Nml $CH_4/g_{VS}$/day, while GSp peaked on the second day with 21.5 Nml $CH_4/g_{VS}$/day. The rapid increase in methane production during the first days of digestion reflects the fast consumption of readily biodegradable compounds, particularly in FVW. Once the maximum metabolic activity is reached, the rate starts to decline as degradable substrate becomes progressively depleted in the batch system. In the case of GS, the peak appears later probably because

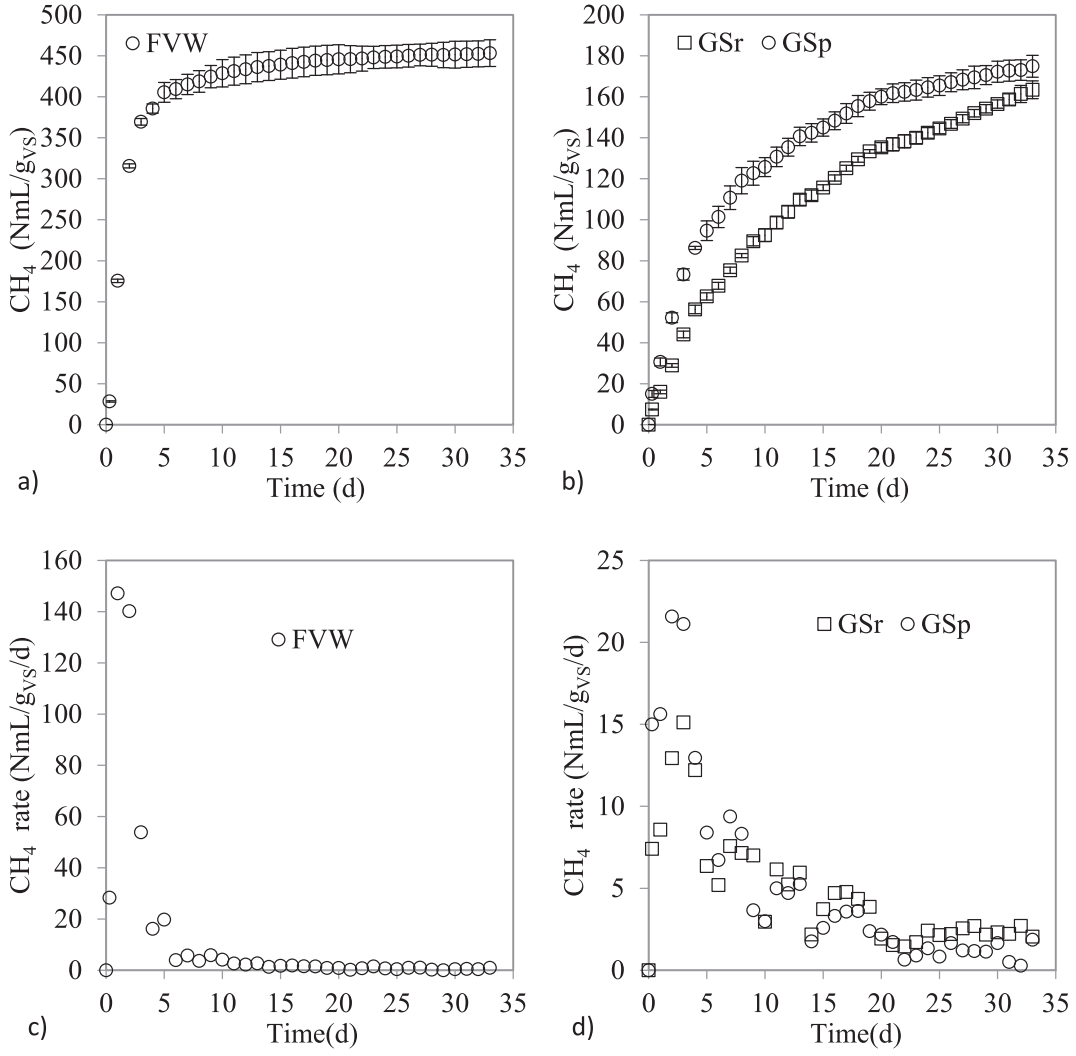


**Fig. 2.** Methane generation and production rate for FVW, GSr, and GSp; (a) and (b) are cumulative volume generation and (c) y (d) are daily productions.

**Table 3**
Experimental and theoretical methane potential results.

| Parameters | FVW | GSr | GSt | GSr: FVW | | | | GSt: FVW | | | |
|---|---|---|---|---|---|---|---|---|---|---|---|
| | | | | 20:80 | 40:60 | 60:40 | 80:20 | 20:80 | 40:60 | 60:40 | 80:20 |
| $BMP_{exp}$ ($NmlCH_4/g_{VS}$) | 453 | 163 | 175 | 272 | 204 | 181 | 178 | 271 | 207 | 186 | 183 |
| $BMP_{theo}$ ($NmlCH_4/g_{VS}$) | 464 | 410 | 410 | 433 | 422 | 416 | 413 | 433 | 422 | 416 | 413 |
| BDI (%) | 97.7 | 39.8 | 42.6 | 62.9 | 46.1 | 43.5 | 43.3 | 62.6 | 46.0 | 44.6 | 44.3 |
| Co-digestion performance index (CPI) | – | – | – | 0.96 | 0.91 | 0.93 | 1.02 | 0.93 | 0.89 | 0.91 | 0.98 |
| Final pH | 7.63 | 7.55 | 7.67 | 7.75 | 7.65 | 7.58 | 7.68 | 7.58 | 7.64 | 7.54 | 7.59 |
| Removal of volatile solids (VS) (%) | 81 | 57 | 73 | 67 | 61 | 60 | 58 | 76 | 74 | 74 | 73 |

hydrolysis of its lignocellulosic structure is slower, and the improvement observed for GSp confirms that reducing particle size accelerates hydrolysis and advances the onset of maximum activity. (Jomnonkhaow et al., 2021). Although the methane production rate increases during the first days, this trend does not imply a kinetic lag phase, since biogas generation begins immediately and no clear adaptation delay can be identified. Nevertheless, the significance of this period will be studied with the interpretation of the models results.

The small increase observed in BDI is probably indicating that the methane production has not completely finished. The standard criterion for terminating the test was followed, requiring the daily biogas rate to be equivalent to only 1% of the total volume of biogas produced up to that time. Apparently, for GS digestion, this criterion is not enough, and the experiment should be extended further in time. Again, the model results will be used for a better understanding of this issue.

The CPI is influenced by factors such as the feedstock's type and ratio, the feedstock's quality, and the digester's operating conditions. (Phuttaro et al., 2023; Rangseesuriyachai et al., 2023). If the co-digestion enhances the methane production with respect to the separated digestion of each substrate, the CPI value would be above 1, driven by interactions between substrates that mitigate inhibitory factors affecting AD. Conversely, when the CPI is below 1, the process is deemed antagonistic, indicating diminished performance (Hou et al., 2020). CPI values indicate additive behavior when CPI = 1. In Table 3, the CPI index ranged from 0.89 to 1.02, with no clear trend as the ratio of GS to FVW increases. All CPI values remained close to 1, confirming strictly

additive behavior for the AcoD of the two residues with quite different lignocellulosic content.

While synergistic effects related to nutrient balance cannot be reliably assessed using BMP tests (Koch et al., 2020; VDI *4630*, 2016), BMP assays remain widely used to detect other forms of synergism. Several studies have reported synergism in AcoD using BMP assays (Awais et al., 2016; Ma et al., 2019). Notably, BMP is effective for identifying synergism arising from complementary biochemical composition (Astals et al., 2014; Cucina et al., 2021), where mixtures of substrates with different carbon fractions (e.g., carbohydrates, proteins, lipids) enhanced methane production.

The final pH values of the control, mono-substrates, and mixtures ranged between 7.6 and 7.9, slightly above the initial pH value of the inoculum, consistent with findings reported in the literature for BMP assays.

The removal of VS after 33 days of digestion in the BMP assays was calculated by comparing the initial VS content of the inoculum and each substrate individually with the VS content of the digestate at the end of the assays. In the control assays, VS removal was approximately 36%, indicating that the inoculum itself contained biodegradable material. Table 3 shows that the highest VS removal was observed for FVW, followed by GSp and GSr. This trend aligns with the BDI results, although the differences are less pronounced, likely due to the high inoculum-to-substrate VS ratio (4:1) used in the tests. With approximately 12 g of VS from the inoculum and only 3 g from the substrate, any error in measuring the inoculum's VS content is amplified in the calculation of

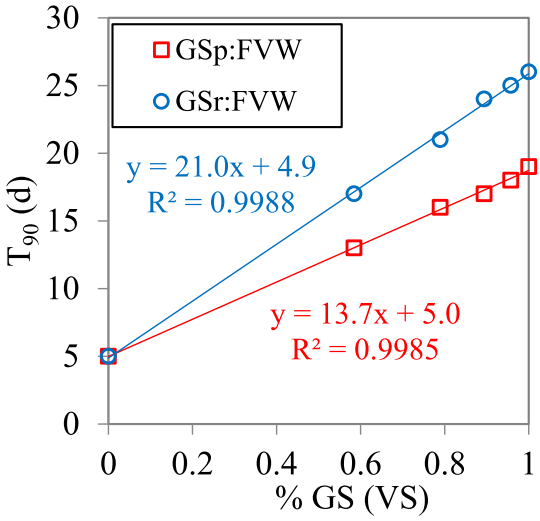


**Fig. 4.** $T_{90}$ for different GS:FVW ratios referred to VS.

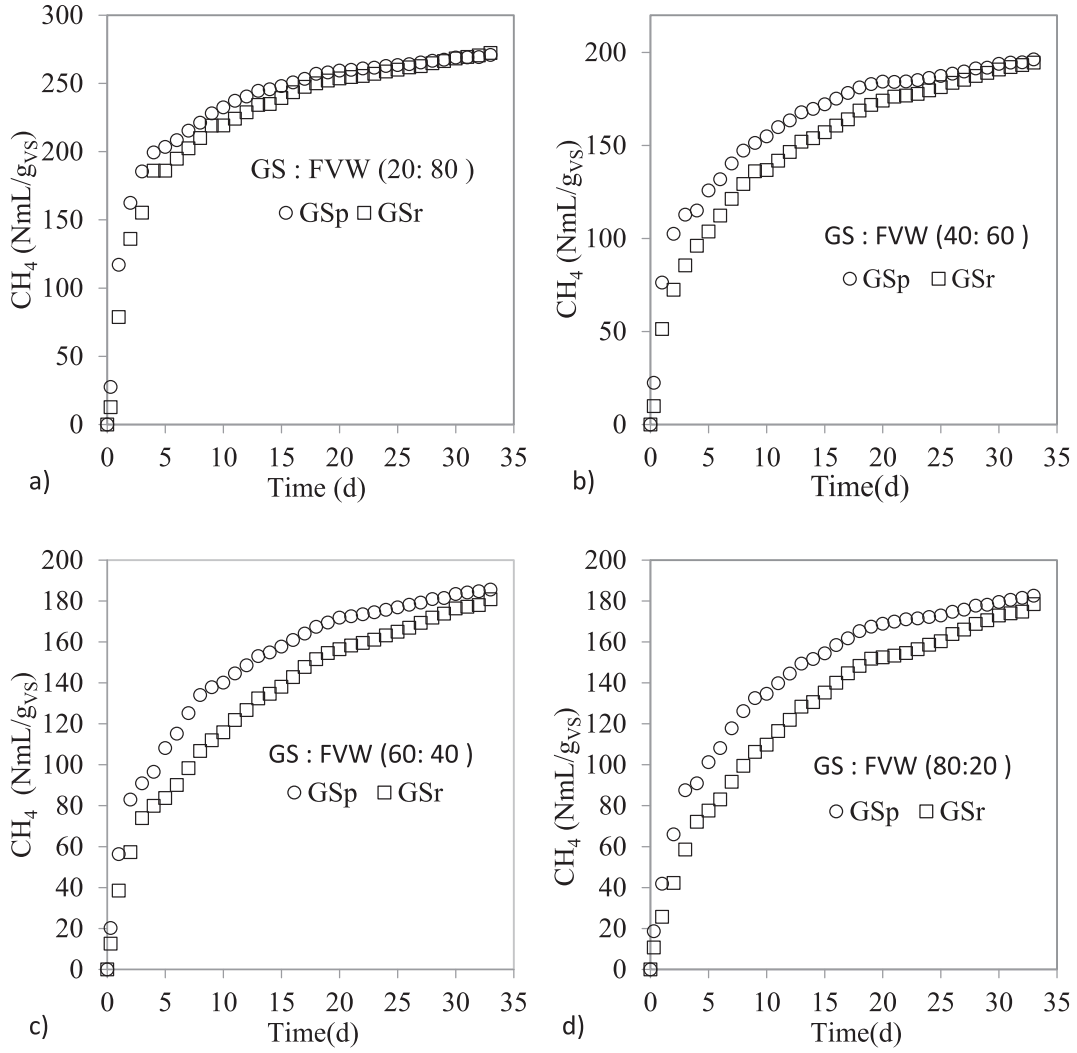


**Fig. 3.** Effect of pretreatment and co-digestion on accumulated biochemical methane production for mixtures at mass ratio of GS:FVW: (a) 20:80, (b) 40:60, (c) 60:40, (d) 80:20. Results are shown for both GSr and GSp.

substrate-specific VS removal. For the co-digestion mixtures, removal values were estimated by a weighted linear combination of the individual VS removal values, based on their proportions in the mixtures. While these values are consistent with the BDI trends, they should be interpreted with care due to the uncertainties discussed above.

An important parameter derived from BMP data is the technical digestion time ($T_{90}$), defined as the time required to reach 90% of the maximum methane production. This metric is essential for estimating the hydraulic retention time (HRT) in continuous AD systems (Kafle and Chen, 2016). For FVW, $T_{90}$ was achieved within just 5 days, reflecting its high content of readily biodegradable material. In contrast, GSr and GSp reached $T_{90}$ after 26 and 19 days, respectively, indicating slower degradation. These results suggest that particle size reduction through pretreatment would probably reduce the HRT in a continuous digester.

The results of co-digestion involving various mixtures of FVW, GSr, and GSp are presented in Fig. 3. Methane production started on the first day in all digesters. The maximum daily methane production rates increased with the proportion of FVW in the mixture. Specifically, the mixtures containing GSp and FVW exhibited higher maximum daily methane production rates than those containing GSr and FVW. Moreover, the methane production kinetics were faster for the GSp mixtures. However, reducing the grass particle size (GSr) did not significantly affect the observed BMP values.

As expected, $T_{90}$ increased with the proportion of GS in the mixture, regardless of whether the grass was pretreated or not. This behavior aligns with the relationship between $T_{90}$ and HRT discussed earlier, indicating that HRT increases would be required with increases of the GS:FVW ratio. Fig. 4 shows the $T_{90}$ values plotted against the GS:FVW ratio, expressed in terms of VS. A linear increase in $T_{90}$ is observed, with $R^2$ values exceeding 0.998 for both cases. The slope for the mixtures of GSp with FVW is approximately 50% higher than that for the GSr and FVW mixtures. The linearity of these results supports the previous observation of additive co-digestion behavior.

### 3.3. Theoretical BMP

The $BMP_{theo}$ of FVW, GS, and their mixtures was estimated using modified Buswell and Mueller's equation (Eq. 1). Table 3 compares different substrates' experimental and theoretical BMP. The $BMP_{theo}$, calculated based on elemental analysis, assumes that the substrate's carbon, hydrogen, nitrogen, sulfur, and oxygen atoms are fully converted to biogas, with minor traces of other compounds.

Table 3 shows that the experimental and theoretical BMP values are closely aligned for the FVW samples, whereas significant discrepancies are observed for all other samples. The BDI is approximately 98% for FVW but ranges between 39% and 63% for all the samples containing grass. The BMP experiments were conducted following the standard procedure, in which each test is concluded when the daily biogas production falls below 1% of the cumulative volume produced up to that point. However, the results for the grass-containing samples reveal a clear discrepancy between the $BMP_{theo}$ and the values obtained using the standard experimental method. Based on subsequent analysis of methane production kinetics, the criterion used to terminate the BMP tests may not be sufficient to fully capture the methane potential of these substrates. As will be discussed later, the use of kinetic modeling provides a valuable tool for interpreting BMP results and may help to resolve these discrepancies.

The overestimation of BMP for GSr and GSp likely arises from the assumption in the $BMP_{theo}$ calculation that all organic matter is readily degradable, which does not reflect actual conditions. Not all organic matter in the substrates can be degraded during experimental time. The higher BDI observed for FVW is attributable to its greater proportion of readily biodegradable organic matter.

### 3.4. BMP modeling

The evolution of methane production over time for each case was modeled using six different kinetic models: FO, TFFO, MT, MG, S, and MS models (Eqs. 5–10). The kinetic parameters were estimated using the Solver add-in of Microsoft Excel (Microsoft Office 365) by global least-squares minimization of the sum of squared errors (SEE) between measured and predicted cumulative methane production across all mono- and co-digestion assays simultaneously. Because the co-digestion experiments involving GSr and GSp represent two independent experimental datasets, two separate global optimizations were carried out: one for all GSr-FVW assays and another for all GSp-FVW assays. Each optimization simultaneously included the six experimental curves corresponding to the mono-digestion of FVW and GS (GSr or GSp) and their four co-digestion mixtures. In practice, the objective function minimized the SEE calculated over all experimental data points (35 time-points × 6 assays, per optimization). As demonstrated experimentally (CPI values close to 1 for all eight AcoD assays, shown in Table 3), the co-digestion of GS and FVW followed a strictly additive behavior, with the methane yields of the mixtures corresponding to the VS-weighted sum of the mono-digestion contributions. To confirm that this additive behavior persisted over time, an instantaneous CPI was calculated at each sampling point using Eq. (4) with cumulative methane production, $V_{CH_4}(t)$, instead of BMP. The mean instantaneous CPI across all AcoD assays was $0.95 \pm 0.09$ for GSr:FVW co-digestions and $0.97 \pm 0.07$ for GSp:FVW co-digestions, confirming that the additive behavior was consistently maintained throughout the entire co-digestion period.

As long as these conditions are true, co-digestion would proceed as two parallel and independent degradation processes, and therefore only two sets of kinetic parameters (one for FVW and one for each GS) would be required to describe the entire dataset. The predicted methane production of each mixture was calculated from the VS-weighted combination of the predicted mono-digestion curves. For a mixture prepared on a wet-weight ratio of X:Y, the predicted methane production was calculated as

$$V_{CH_4}^{X:Y} = \frac{VS_{GS}\cdot X}{VS_{GS}\cdot X + VS_{FVW}\cdot Y} V_{CH_4}^{X:0} + \frac{VS_{FVW}\cdot Y}{VS_{GS}\cdot X + VS_{FVW}\cdot Y}\, V_{CH_4}^{0:Y} \tag{14}$$

Where $V_{CH_4}^{X:Y}$ is the predicted co-digestion methane production of the mixture with wet-weight ratio X:Y; X and Y represent the wet weights of GS and FVW, respectively; $VS_{GS}$ and $VS_{FVW}$ are their corresponding volatile solids contents; $V_{CH_4}^{X:0}$ is the methane volume predicted for mono-digestion of GS; and $V_{CH_4}^{0:Y}$ is the methane volume predicted for mono-digestion of FVW.

This global regression approach avoids overfitting individual mixtures and enforces the additive constraint derived from the experimental data. The AIC was then used to identify the model that best describes the experimental data.

The FO and MT models adequately reproduced the experimental data for FVW mixtures with both GSr and GSp (Fig. 5a,c and Fig. 6a,c). However, this was only achieved when all four fitting parameters were utilized: the two kinetics constants and the two BMPs for GS and FVW. Their performance significantly fails when the number of fitting parameters is reduced to two by setting the BMP values of the individual wastes for the model as those theoretically predicted by CHNSO analysis (not shown). This failure is probably related to low BDI values. Similarly, the MG model also failed to provide an adequate fit when the BMP values were set as those predicted by CHNSO analysis. An adequate fit was only obtained when all six fitting parameters were used, including BMP, maximum rate constant, and lag time for both individual wastes (Fig. 5d and Fig. 6d). For the S model, constraining the sum of BMPs from the easily and poorly biodegradable substrates to the values predicted by CHNSO analysis did not yield a satisfactory fit. Only by adjusting all ten fitting parameters (including, for each substrate, BMPs, first-order and maximum rate constants, and lag times) was the model

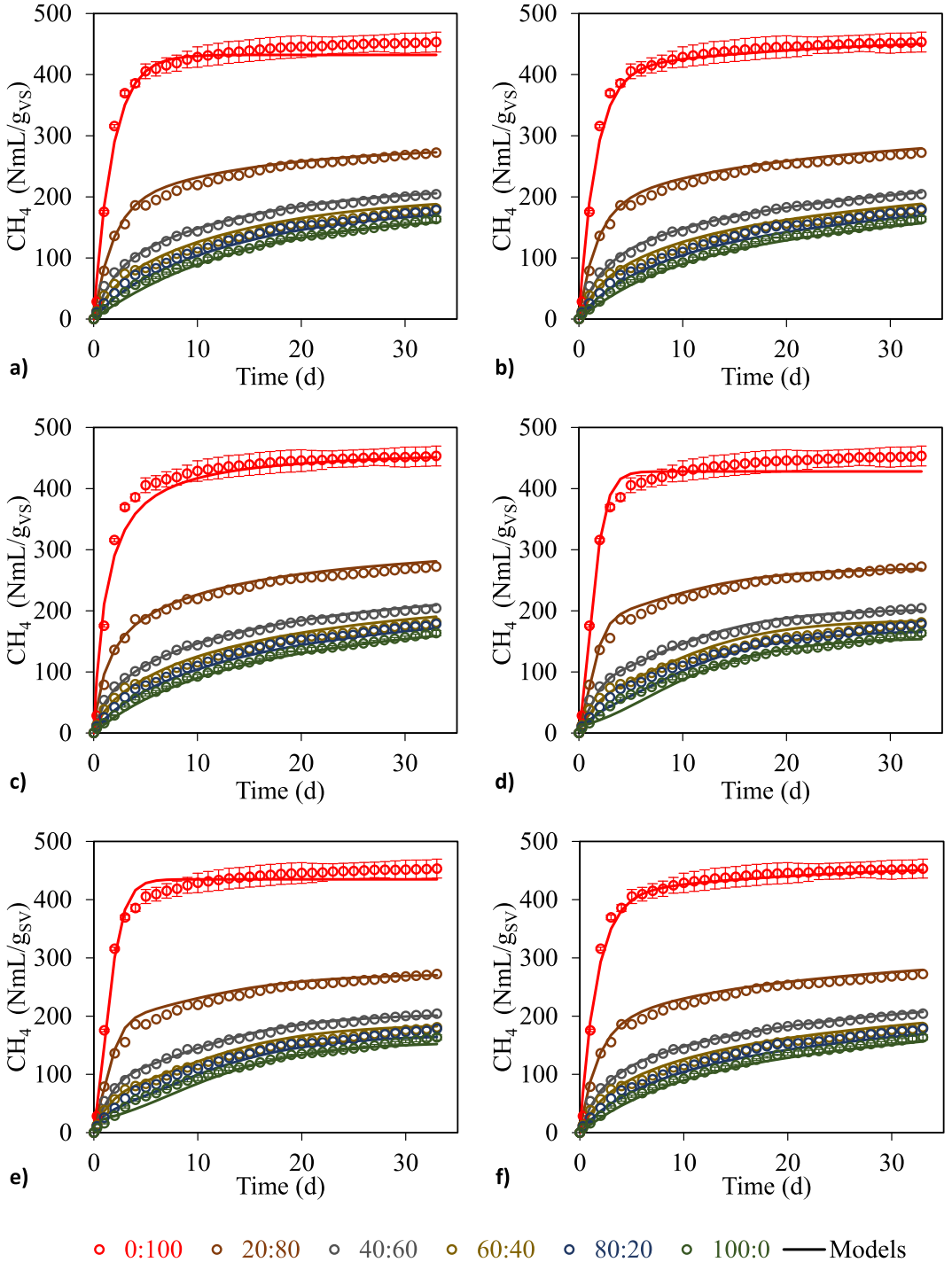


**Fig. 5.** Fitting results of the six models for mixtures of FVW and raw grass: (a) FO, (b) TFFO, (c) MT, (d) MG, (e) S, (f) MS. Mass ratio expressed as GSr:FVW.

able to accurately reproduce the observed data (Fig. 5e and Fig. 6e). This suggests that these models lack the necessary flexibility to describe the complex biodegradation dynamics of GS and FVW, particularly when the BMP values are not used as fitting parameters but are instead fixed to their theoretical values derived from elemental analysis.

Although the MG model did not reproduce the experimental results satisfactorily, it is noteworthy that the maximum methane production rate ($R_m$) of GSp was approximately 1.6 times higher than that of GSr. This finding indicates that particle-size reduction enhances substrate accessibility and accelerates the initial hydrolysis dynamics of grass biodegradation. Both GSr and GSp exhibited negligible lag times, suggesting that microbial colonization is not delayed in either case, while a lag phase of approximately 2.5 h was predicted for FVW. Although the MG model is often adopted for its empirical sigmoidal response and explicit lag parameter, its suitability decreases when substrates include a substantial slowly-degradable fraction. For lignocellulosic or heterogeneous wastes, several studies report improved fitting performance using dual-pool, multi-stage or hybrid models (Brulé et al., 2014; Undiandeye et al., 2022).

In the case of the S model, the first-order component resulted in an extremely high rate constant ($k = 174\ d^{-1}$ for all substrates), rendering its contribution to methane production negligible. Under these conditions, the S model becomes mathematically dominated by the Gompertz-type term, leading to predictions close to those of the MG model but still

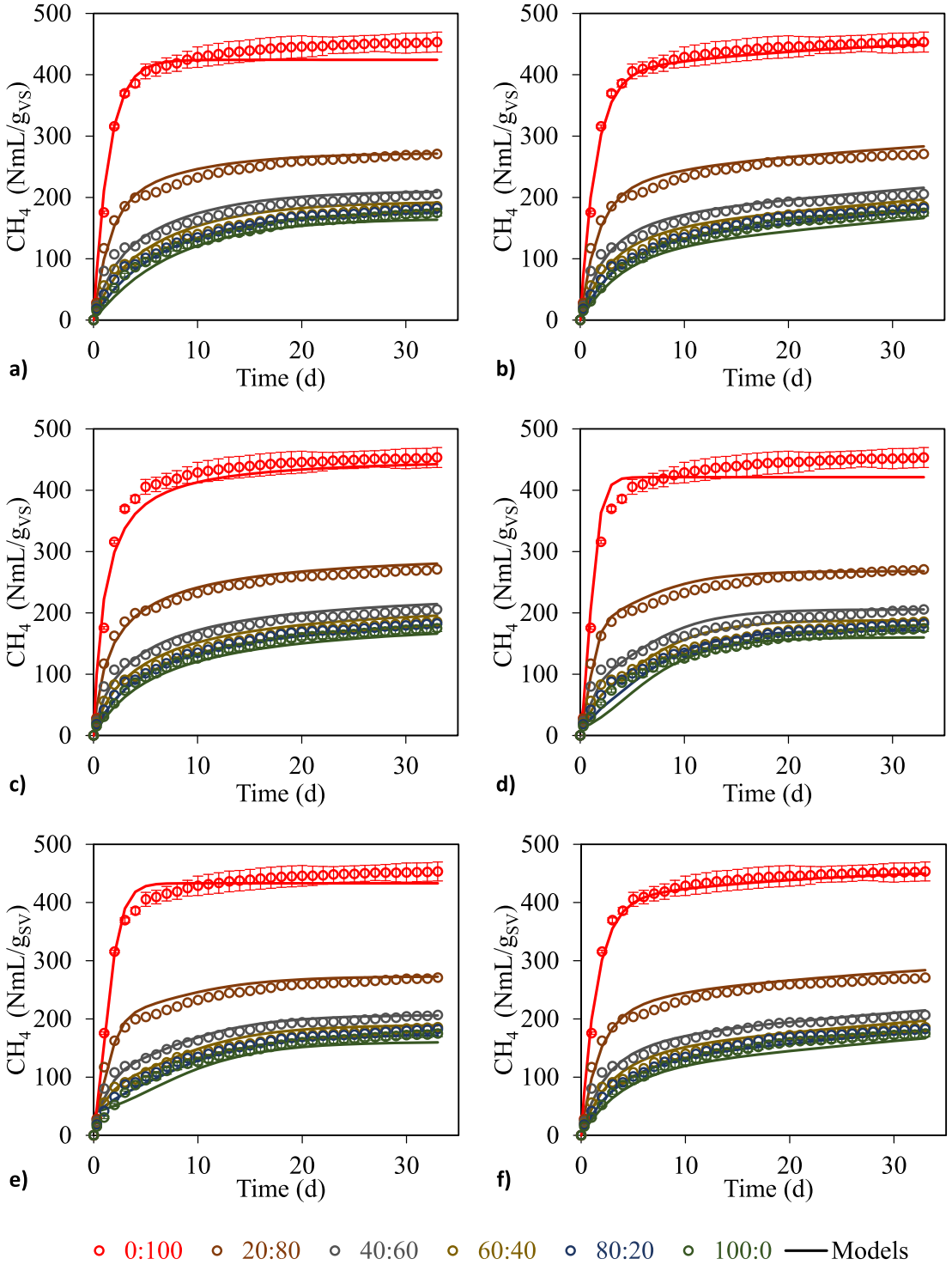


**Fig. 6.** Fitting results of the six models for mixtures of FVW and pre-treated grass: (a) FO, (b) TFFO, (c) MT, (d) MG, (e) S, (f) MS. Mass ratio expressed as GSp:FVW.

failing to capture key experimental trends. In particular, the increase in $R_m$ between GSr and GSp is reduced to only 1.15, and the lag time for GSr increases to about 2.5 h. These discrepancies further confirm that MG and S models do not adequately represent the kinetics of this system.

In contrast, based on the AIC, the TFFO and MS models exhibited the best performance to the experimental data for FVW mixtures with both GSr and GSp. Table 4 presents the AIC values for the six models (12 fits), along with the corresponding fitted model parameters. The TFFO kinetic model performed noticeably better, yielding lower AIC values, when the number of fitting parameters was reduced from eight to six by fixing the BMP values to those predicted from CHNSO analysis (Fig. 5b and Fig. 6b). Similarly, the MS kinetic model also improved when the number parameters was reduced from ten to eight (Fig. 5f and Fig. 6f). This reduction was achieved by constraining the sum of the three BMPs (two stages and their interaction) to the values predicted from CHNS analysis of each substrate. TFFO and MS models account for both fast and slow biodegradable fractions/stages of GS and FVW, along with distinct rate constants for each fraction/stages, thereby capturing the heterogeneous behavior of these organic residues more effectively.

Both the TFFO and MS models provided excellent fits to the experi-

**Table 4**
Model parameter values derived from fitting to experimental data. Bold values denote the best-fitting models based on AIC.

| Model | | | GSr:FVW mixtures | | GSp:FVW mixtures | |
|---|---|---|---|---|---|---|
| | | | GSr | FVW | GSp | FVW |
| First-order | BMP | $(NmL\ g_{SV}^{-1})$ | 175 | 432 | 166 | 424 |
| | $k_1$ | $(d^{-1})$ | 0.071 | 0.555 | 0.131 | 0.688 |
| | RMSE | $(NmL\ g_{SV}^{-1})$ | 8.200 | | 13.221 | |
| | $R^2$ | | 0.984 | | 0.989 | |
| | AIC | | 891 | | 1091 | |
| Two fractions first-order | BMP* | $(NmL\ g_{SV}^{-1})$ | 410 | 464 | 410 | 464 |
| | α | (−) | 0.25 | 0.87 | 0.27 | 0.86 |
| | $k_f$ | $(d^{-1})$ | 0.12 | 0.62 | 0.25 | 0.68 |
| | $k_s$ | $(d^{-1})$ | 0.006 | 0.044 | 0.006 | 0.045 |
| | RMSE | $(NmL\ g_{SV}^{-1})$ | 7.369 | | 9.330 | |
| | $R^2$ | | 0.988 | | 0.951 | |
| | AIC | | **850** | | **949** | |
| Monod type | BMP | $(NmL\ g_{SV}^{-1})$ | 238 | 468 | 199 | 457 |
| | k | $(d^{-1})$ | 0.060 | 0.819 | 0.154 | 0.948 |
| | RMSE | $(NmL\ g_{SV}^{-1})$ | 9.205 | | 10.490 | |
| | $R^2$ | | 0.988 | | 0.952 | |
| | AIC | | 877 | | 994 | |
| Modified Gompertz | BMP | $(NmL\ g_{SV}^{-1})$ | 156 | 428 | 160 | 421 |
| | $R_m$ | $(NmL\ g_{SV}^{-1}\ d^{-1})$ | 8.83 | 187 | 14.06 | 247 |
| | λ | $(d^{-1})$ | 0 | 0.172 | 0 | 0.170 |
| | RMSE | $(NmL\ g_{SV}^{-1})$ | 9.974 | | 12.959 | |
| | $R^2$ | | 0.964 | | 0.907 | |
| | AIC | | 977 | | 1087 | |
| Superimposed | $BMP_1$ | $(NmL\ g_{SV}^{-1})$ | 10.3 | 0 | 30.9 | 0 |
| | $BMP_2$ | $(NmL\ g_{SV}^{-1})$ | 146 | 435 | 130 | 433 |
| | k | $(d^{-1})$ | 174 | 174 | 174 | 174 |
| | $R_m$ | $(NmL\ g_{SV}^{-1}\ d^{-1})$ | 7.53 | 171 | 8.69 | 181 |
| | λ | $(d^{-1})$ | 0.104 | 0.135 | 0 | 0.135 |
| | RMSE | $(NmL\ g_{SV}^{-1})$ | 9.675 | | 11.135 | |
| | $R^2$ | | 0.971 | | 0.927 | |
| | AIC | | 972 | | 1031 | |
| Multi-stage | $BMP_S$ | $(NmL\ g_{SV}^{-1})$ | 108 | 408 | 115 | 402 |
| | $BMP_I$ | $(NmL\ g_{SV}^{-1})$ | 243 | 35 | 83 | 43 |
| | $BMP_{IS}$ | $(NmL\ g_{SV}^{-1})$ | 60 | 21 | 212 | 19 |
| | $k_1$ | $(d^{-1})$ | 0.12 | 0.62 | 0.25 | 0.67 |
| | $k_2$ | $(d^{-1})$ | 0.006 | 0.045 | 0.006 | 0.046 |
| | RMSE | $(NmL\ g_{SV}^{-1})$ | 7.369 | | 9.330 | |
| | $R^2$ | | 0.988 | | 0.951 | |
| | AIC | | **854** | | **953** | |

mental cumulative methane curves, with nearly indistinguishable statistical performance. Surprisingly, the kinetic parameters estimated independently for each model showed an almost perfect correspondence. The values of the fast and slow degradation rate coefficients in the TFFO model ($k_f$,$k_s$) closely matched $k_1$ and $k_2$, respectively, from the MS model. To clarify the origin of this correspondence, a mathematical demonstration was conducted showing that the analytical expression of the MS model (Eq. 9) can be rearranged into the TFFO formulation (Eq. 6). This demonstration, provided in the Supplementary Material, indicates that the partitioning coefficient α of the TFFO model is directly related to the MS kinetic parameters according to:

$$\alpha = \frac{\left(BMP_S + BMP_{IS}\frac{k_2}{k_2 - k_1}\right)}{(BMP_S + BMP_I + BMP_{IS})} \quad (15)$$

Applying this expression to the MS kinetic parameters reported in Table 4 results in α values identical to those obtained from the TFFO fitting, for both GS and FVW, thereby confirming the mathematical equivalence of both kinetic formulations.

In addition to the global fitting strategy, individual regressions were also performed for each mono- and co-digestion assay to evaluate model behavior without additive constraints. The resulting parameter sets and statistical indicators (AIC, RMSE, and $R^2$) are provided in the Supplementary Material (Section S3, Tables 2-S to 4-S, and Figs. 1-S to 5-S). These individual fits confirm the conclusions of the global optimization: the TFFO/MS models consistently yielded the best quantitative performance, whereas FO, MG, and S models showed limited predictive capability, particularly under co-digestion conditions.

As shown in Table 4, the identical fast-biodegradable fraction obtained for each pure substrate in both independent global optimizations (GSr or GSp with FVW) confirms the internal consistency of the kinetic model and demonstrates that parameter estimation is unaffected by the inclusion of the co-digestion datasets in the global optimization. However, this is not the case for the kinetic coefficients. The kinetic coefficient of the fast-biodegradable fraction of GSp is approximately twice that of GSr. In contrast, the pretreatment does not appear to affect the slow-biodegradation kinetics, as the kinetic coefficient remains nearly identical for GSr and GSp. For FVW, as expected in a additive process, the values of both kinetic constants remain unaffected by the pretreatment applied to the other waste in the mixture.

The regression equations proposed by Alrefaey et al. (2024) for predicting kinetic parameters in lignocellulosic wastes were applied to estimate the FO and MG parameters for the GS and FVW. However, the predicted kinetic parameters were markedly different from the values obtained experimentally, raising concerns about the reliability of the regression approach. To assess whether this discrepancy was specific to the substrates or inherent to the regression model itself, the same equations were then applied to the experimental data reported by the authors for their S1 and S2 substrates (rice straw from different Egyptian regions). In this validation step, the predicted regression values also failed to reproduce the reported rate constant for the FO model and the lag phase for the MG model, suggesting possible inconsistencies in the published coefficients or parameter definitions. Due to this lack of agreement, the regressions were not extended to the remaining substrates (S3–S10) or to the mixtures tested in the present work. Furthermore, statistical criteria for model selection were not provided in their study, making it difficult to assess the robustness of each kinetic formulation.

Overall, the results highlight the significance of selecting an appropriate kinetic model to accurately describe the evolution of the biomethane volume produced in AD systems. The TFFO and MS models, with their ability to differentiate between fast and slow degradation fractions/stages while incorporating theoretical BMP predictions, provide a robust framework for predicting methane production from mixed organic residues with additive, non-synergistic interactions.

As indicated previously in Section 3.2, the standard procedure for obtaining the BMP may fail with samples containing grass because the termination criterion appears to yield a time too small to capture the full BMP. The TFFO and MS kinetic models indicate that the slow fraction is too slow to be measured within the experimental time determined by the standard procedure. As a matter of fact, to obtain the release of 90% of the theoretical BMP the experimental time needed would be of about a year, as predicted from the models. Nevertheless, the terminating-time criterium of the standard procedure is good enough as long as the results are interpreted with this model.

The relationship between the fast biodegradable fraction of a waste and its fiber composition could provide valuable insights into the biodegradability of different organic residues. As can be shown in Table 2, grass residue contains more hemicellulose, cellulose, and lignin (91%) than FVW (8%). These compounds likely limit the biodegradation rate, as microorganisms must first break down their rough structures before they can fully metabolize the organic material. Accordingly, the results indicate that FVW is more readily biodegradable than grass waste. Thus, while grass is a highly available feedstock, its effective

conversion to biogas requires either co-digestion, pretreatment, or substantially longer operating times, as well as further investigation into existing techniques and the development of innovative approaches to enhance its degradability.

## 4. Conclusions

The results of this study demonstrate that FVW is a highly effective co-substrate for AD due to its superior methane yield and biodegradability compared to GS. While mechanical pretreatment of grass through particle size reduction slightly improved the methane production rate, it did not significantly enhance overall methane yield, indicating limited benefits from extensive grinding. Co-digestion of GS and FVW at various ratios yielded additive behavior, as reflected by CPI values close to unity. Notably, BMP values for grass-containing substrates fell short of theoretical predictions, underscoring the limitations of standard BMP test durations when dealing with slowly degradable lignocellulosic material. Kinetic modeling proved essential for resolving these discrepancies, with the TFFO and MS models emerging as the most effective at capturing the dynamics of methane production. Although these models are conceptually different, they yield mathematically identical kinetic expressions for methane production. By distinguishing between fast and slow degradation phases/stages, these models not only offered the best fit to experimental data but also provided a more realistic representation of substrate behavior. These findings highlight the need to complement standard BMP assays with kinetic modeling, particularly when evaluating complex or recalcitrant substrates, to improve the design, prediction, and optimization of AD systems.

## CRediT authorship contribution statement

**Brahim Arhoun:** Writing – original draft, Investigation, Data curation, Conceptualization. **Belén Muñoz-Cabello:** Methodology, Investigation, Data curation. **Souad Benaisa:** Methodology, Investigation. **Cesar Gomez-Lahoz:** Writing – review & editing, Formal analysis, Conceptualization. **Carlos Vereda-Alonso:** Formal analysis, Data curation, Conceptualization. **María del Mar Cerrillo-González:** Formal analysis, Data curation.

## Declaration of competing interest

The authors declare that they have no known competing financial interests or personal relationships that could have appeared to influence the work reported in this paper.

## Acknowledgments

The authors acknowledge the financial funding from the State plan for scientific, technical, and innovation research from The Ministry of Science and Innovation of Spain [grant number TED2021-130756B-C31].

The authors also acknowledge the financial funding from the regional government Junta de Andalucía [PPRO-RNM-281-G-FEDER-2023].

Funding for open access charge: Universidad de Málaga/CBUA

## Appendix A. Supplementary data

Supplementary data to this article can be found online at https://doi.org/10.1016/j.biteb.2026.102597.

## Data availability

Data will be made available on request.

## References

Aguilar-Aguilar, F.A., Mena-Cervantes, V.Y., Mederos-Nieto, F.S., Pineda-Flores, G., Morales-García, S.S., Hernández-Altamirano, R., 2025. Biochemical methane potential of coyol fruit as a substrate for biogas production through mixture design and kinetic modeling. Biomass Bioenergy 193, 107571. https://doi.org/10.1016/j.biombioe.2024.107571.

Almeida, P.V., Rodrigues, R.P., Mendes, C.V.T., Szeląg, R., Pietrzyk, D., Klepacz-Smółka, A., Quina, M.J., 2021. Assessment of NIR spectroscopy for predicting biochemical methane potential of agro-residues – a biorefinery approach. Biomass Bioenergy 151, 106169. https://doi.org/10.1016/j.biombioe.2021.106169.

Alrefaey, K., Schultz, J., Scherzinger, M., Nosier, M.A., Elbanhawy, A.Y., 2024. Prediction of anaerobic degradation kinetics based on substrate composition of lignocellulosic biomass. Bioresour. Technol. Rep. 27, 101882. https://doi.org/10.1016/j.biteb.2024.101882.

Arhoun, B., Villen-Guzman, M.D., Vereda-Alonso, C., Rodriguez-Maroto, J.M., Garcia-Herruzo, F., Gómez-Lahoz, C., 2019. Anaerobic co-digestion of municipal sewage sludge and fruit/vegetable waste: effect of different mixtures on digester stability and methane yield. J. Environ. Sci. Health A 1–7. https://doi.org/10.1080/10934529.2019.1579523.

Astals, S., Batstone, D.J., Mata-Alvarez, J., Jensen, P.D., 2014. Identification of synergistic impacts during anaerobic co-digestion of organic wastes. Bioresour. Technol. 169, 421–427. https://doi.org/10.1016/j.biortech.2014.07.024.

Awais, M., Alvarado-Morales, M., Tsapekos, P., Gulfraz, M., Angelidaki, I., 2016. Methane production and kinetic modeling for co-digestion of manure with lignocellulosic residues. Energy Fuel 30, 10516–10523. https://doi.org/10.1021/acs.energyfuels.6b02105.

Brulé, M., Oechsner, H., Jungbluth, T., 2014. Exponential model describing methane production kinetics in batch anaerobic digestion: a tool for evaluation of biochemical methane potential assays. Bioprocess Biosyst. Eng. 37, 1759–1770. https://doi.org/10.1007/s00449-014-1150-4.

Burnham, K.P., Anderson, D.R., 2004. Model selection and multimodel inference. Springer New York, New York, NY. https://doi.org/10.1007/b97636.

Butkutė, B., Lemežienė, N., Kanapeckas, J., Navickas, K., Dabkevičius, Z., Venslauskas, K., 2014. Cocksfoot, tall fescue and reed canary grass: dry matter yield, chemical composition and biomass convertibility to methane. Biomass Bioenergy 66, 1–11. https://doi.org/10.1016/j.biombioe.2014.03.014.

Cucina, M., Pezzolla, D., Tacconi, C., Gigliotti, G., 2021. Anaerobic co-digestion of a lignocellulosic residue with different organic wastes: relationship between biomethane yield, soluble organic matter and process stability. Biomass Bioenergy 153, 106209. https://doi.org/10.1016/j.biombioe.2021.106209.

D' Silva, T.C., Isha, A., Verma, S., Shirsath, G., Chandra, R., Vijay, V.K., Subbarao, P.M. V., Kovács, K.L., 2022. Anaerobic co-digestion of dry fallen leaves, fruit/vegetable wastes and cow dung without an active inoculum – a biomethane potential study. Bioresour. Technol. Rep. 19, 101189. https://doi.org/10.1016/j.biteb.2022.101189.

Di Maria, F., Sordi, A., Cirulli, G., Micale, C., 2015. Amount of energy recoverable from an existing sludge digester with the co-digestion with fruit and vegetable waste at reduced retention time. Appl. Energy 150, 9–14. https://doi.org/10.1016/j.apenergy.2015.01.146.

Dickeduisberg, M., Laser, H., Tonn, B., Isselstein, J., 2017. Tall wheatgrass (*Agropyron elongatum*) for biogas production: crop management more important for biomass and methane yield than grass provenance. Ind. Crop. Prod. 97, 653–663. https://doi.org/10.1016/j.indcrop.2016.12.055.

Ebner, J.H., Labatut, R.A., Lodge, J.S., Williamson, A.A., Trabold, T.A., 2016. Anaerobic co-digestion of commercial food waste and dairy manure: characterizing biochemical parameters and synergistic effects. Waste Manag. 52, 286–294. https://doi.org/10.1016/j.wasman.2016.03.046.

Edwiges, T., Frare, L., Mayer, B., Lins, L., Mi Triolo, J., Flotats, X., de Mendonça Costa, M. S.S., 2018. Influence of chemical composition on biochemical methane potential of fruit and vegetable waste. Waste Manag. 71, 618–625. https://doi.org/10.1016/j.wasman.2017.05.030.

Edwiges, T., Bastos, J.A., Lima Alino, J.H., d'avila, L., Frare, L.M., Somer, J.G., 2019. Comparison of various pretreatment techniques to enhance biodegradability of lignocellulosic biomass for methane production. J. Environ. Chem. Eng. 7, 103495. https://doi.org/10.1016/j.jece.2019.103495.

Egwu, U., Onyelowe, K., Tabraiz, S., Johnson, E., Mutshow, A.D., 2022. Investigation of the effect of equal and unequal feeding time intervals on process stability and methane yield during anaerobic digestion grass silage. Renew. Sust. Energ. Rev. 158, 112092. https://doi.org/10.1016/j.rser.2022.112092.

El Gnaoui, Y., Frimane, A., Lahboubi, N., Herrmann, C., Barz, M., EL Bari, H., 2022. Biological pre-hydrolysis and thermal pretreatment applied for anaerobic digestion improvement: kinetic study and statistical variable selection. Clean. Waste Syst 2, 100005. https://doi.org/10.1016/j.clwas.2022.100005.

García-Gen, S., Sousbie, P., Rangaraj, G., Lema, J.M., Rodríguez, J., Steyer, J.-P., Torrijos, M., 2015. Kinetic modelling of anaerobic hydrolysis of solid wastes, including disintegration processes. Waste Manag. 35, 96–104. https://doi.org/10.1016/j.wasman.2014.10.012.

Hmeekong, A., Chuenchom, L., Charnnok, B., Chaiprapat, S., 2025. Sustainable valorization of grass biomass via hydrothermal pretreatment for biogas and biofuel co-production. J. Environ. Manag. 389, 126109. https://doi.org/10.1016/j.jenvman.2025.126109.

Hou, T., Zhao, J., Lei, Z., Shimizu, K., Zhang, Z., 2020. Synergistic effects of rice straw and rice bran on enhanced methane production and process stability of anaerobic digestion of food waste. Bioresour. Technol. 314, 123775. https://doi.org/10.1016/j.biortech.2020.123775.

Jiang, P., Fan, Y.V., Klemeš, J.J., 2021. Impacts of COVID-19 on energy demand and consumption: challenges, lessons and emerging opportunities. Appl. Energy 285, 116441. https://doi.org/10.1016/j.apenergy.2021.116441.

Jomnonkhaow, U., Sittijunda, S., Reungsang, A., 2021. Influences of size reduction, hydration, and thermal-assisted hydration pretreatment to increase the biogas production from Napier grass and Napier silage. Bioresour. Technol. 331, 125034. https://doi.org/10.1016/j.biortech.2021.125034.

Kafle, G.K., Chen, L., 2016. Comparison on batch anaerobic digestion of five different livestock manures and prediction of biochemical methane potential (BMP) using different statistical models. Waste Manag. 48, 492–502. https://doi.org/10.1016/j.wasman.2015.10.021.

Kang, X., Zhang, Y., Song, B., Sun, Y., Li, L., He, Y., Kong, X., Luo, X., Yuan, Z., 2019. The effect of mechanical pretreatment on the anaerobic digestion of *Hybrid Pennisetum*. Fuel 252, 469–474. https://doi.org/10.1016/j.fuel.2019.04.134.

Karki, R., Chuenchart, W., Surendra, K.C., Sung, S., Raskin, L., Khanal, S.K., 2022. Anaerobic co-digestion of various organic wastes: kinetic modeling and synergistic impact evaluation. Bioresour. Technol. 343, 126063. https://doi.org/10.1016/j.biortech.2021.126063.

Koch, K., Hafner, S.D., Weinrich, S., Astals, S., Holliger, C., 2020. Power and limitations of biochemical methane potential (BMP) tests. Front. Energy Res. 8. https://doi.org/10.3389/fenrg.2020.00063.

Kouas, M., Torrijos, M., Schmitz, S., Sousbie, P., Sayadi, S., Harmand, J., 2018. Co-digestion of solid waste: towards a simple model to predict methane production. Bioresour. Technol. 254, 40–49. https://doi.org/10.1016/j.biortech.2018.01.055.

López, S., Dijkstra, J., Dhanoa, M.S., Bannink, A., Kebreab, E., France, J., 2011. A generic multi-stage compartmental model for interpreting gas production profiles. In: Sauvant, D., Van Milgen, J., Faverdin, P., Friggens, N. (Eds.), Modelling Nutrient Digestion and Utilisation in Farm Animals. Academic Publishers, Wageningen, pp. 139–147. https://doi.org/10.3920/978-90-8686-712-7_15.

Ma, X., Yu, M., Yang, M., Gao, M., Wu, C., Wang, Q., 2019. Synergistic effect from anaerobic co-digestion of food waste and Sophora flavescens residues at different co-substrate ratios. Environ. Sci. Pollut. Res. 26, 37114–37124. https://doi.org/10.1007/s11356-019-06399-x.

Mansor, A.M., Lim, J.S., Ani, F.N., Hashim, H., Ho, W.S., 2019. Characteristics of cellulose, hemicellulose and lignin of MD2 pineapple biomass. Chem. Eng. Trans. 72, 79–84. https://doi.org/10.3303/CET1972014.

Massanet-Nicolau, J., Dinsdale, R., Guwy, A., Shipley, G., 2015. Utilising biohydrogen to increase methane production, energy yields an d process efficiency via two stage anaerobic digestion of grass. Bioresour. Technol. 189, 379–383. https://doi.org/10.1016/j.biortech.2015.03.116.

Melts, I., Normak, A., Nurk, L., Heinsoo, K., 2014. Chemical characteristics of biomass from nature conservation management for methane production. Bioresour. Technol. 167, 226–231. https://doi.org/10.1016/j.biortech.2014.06.009.

Meyer, A.K.P., Ehimen, E.A., Holm-Nielsen, J.B., 2014. Bioenergy production from roadside grass: a case study of the feasibility of using roadside grass for biogas production in Denmark. Resour. Conserv. Recycl. 93, 124–133. https://doi.org/10.1016/j.resconrec.2014.10.003.

Mokjatturas, S., Chinwetkitvanich, S., Patthanaissaranukool, W., Polprasert, C., Polprasert, S., 2025. Phosphorus mass flows and economic benefits of food waste management: the case study of selected retail and wholesale fresh markets in Thailand. Clean Techn. Environ. Policy 27, 219–233. https://doi.org/10.1007/s10098-024-02847-6.

Nielfa, A., Cano, R., Fdz-Polanco, M., 2015. Theoretical methane production generated by the co-digestion of organic fraction municipal solid waste and biological sludge. Biotechnol. Rep. 5, 14–21. https://doi.org/10.1016/j.btre.2014.10.005.

Nolan, P., Luostarinen, S., Doyle, E.M., O'Kiely, P., 2016. Anaerobic digestion of perennial ryegrass prepared by cryogenic freezing versus thermal drying methods, using contrasting *in vitro* batch digestion systems. Renew. Energy 87, 273–278. https://doi.org/10.1016/j.renene.2015.10.026.

Nuchdang, S., Vatanyoopaisarn, S., Phalakornkule, C., 2015. Effectiveness of fungal treatment by *Coprinopsis cinerea* and *Polyporus tricholoma* on degradation and methane yields of lignocellulosic grass. Int. Biodeterior. Biodegradation 104, 38–45. https://doi.org/10.1016/j.ibiod.2015.05.015.

Offermanns, L., Tiemeyer, B., Dettmann, U., Rüffer, J., Düvel, D., Vogel, I., Brümmer, C., 2023. High greenhouse gas emissions after grassland renewal on bog peat soil. Agric. For. Meteorol. 331, 109309. https://doi.org/10.1016/j.agrformet.2023.109309.

Phuttaro, C., Krishnan, S., Saritpongteeraka, K., Charnnok, B., Diels, L., Chaiprapat, S., 2023. Integrated poultry waste management by co-digestion with perennial grass: effects of mixing ratio, pretreatments, reaction temperature, and effluent recycle on biomethanation yield. Biochem. Eng. J. 196, 108937. https://doi.org/10.1016/j.bej.2023.108937.

Prochnow, A., Heiermann, M., Plöchl, M., Linke, B., Idler, C., Amon, T., Hobbs, P.J., 2009. Bioenergy from permanent grassland – a review: 1. biogas. Bioresour. Technol. 100, 4931–4944. https://doi.org/10.1016/j.biortech.2009.05.070.

Rangseesuriyachai, T., Boonnorat, J., Glanpracha, N., Khetkorn, W., Thiamngoen, P., Pinpatthanapong, K., 2023. Anaerobic co-digestion of elephant dung and biological pretreated Napier grass: synergistic effect and kinetics of methane production. Biomass Bioenergy 175, 106849. https://doi.org/10.1016/j.biombioe.2023.106849.

Rodrigues, R.P., Rodrigues, D.P., Klepacz-Smolka, A., Martins, R.C., Quina, M.J., 2019. Comparative analysis of methods and models for predicting biochemical methane potential of various organic substrates. Sci. Total Environ. 649, 1599–1608. https://doi.org/10.1016/j.scitotenv.2018.08.270.

Scherzinger, M., Kaltschmitt, M., Elbanhawy, A.Y., 2022. Anaerobic biogas formation from crops' agricultural residues – modeling investigations. Bioresour. Technol. 359, 127497. https://doi.org/10.1016/j.biortech.2022.127497.

Seppälä, M., Paavola, T., Lehtomäki, A., Rintala, J., 2009. Biogas production from boreal herbaceous grasses – specific methane yield and methane yield per hectare. Bioresour. Technol. 100, 2952–2958. https://doi.org/10.1016/j.biortech.2009.01.044.

Song, Y., Pei, L., Chen, G., Mu, L., Yan, B., Li, H., Zhou, T., 2023. Recent advancements in strategies to improve anaerobic digestion of perennial energy grasses for enhanced methane production. Sci. Total Environ. 861, 160552. https://doi.org/10.1016/j.scitotenv.2022.160552.

Sunar, S.L., Kumara, M.K., Oruganti, R.K., Khadka, K.K., Panda, T.K., Bhattacharyya, D., 2025. Pretreatment and anaerobic co-digestion of lignocellulosic biomass: recent developments. Bioresour. Technol. Rep. 30, 102133. https://doi.org/10.1016/j.biteb.2025.102133.

Trujillo-Reyes, Á., Jiménez-Páez, E., Serrano, A., Kassab, G., Fermoso, F.G., Alonso-Fariñas, B., 2023. Comparative life cycle environmental impact assessment of fruit and vegetable waste valorization by anaerobic digestion as an alternative in a mediterranean market. Processes 11, 3397. https://doi.org/10.3390/pr11123397.

Undiandeye, J., Gallegos, D., Lenz, J., Nelles, M., Stinner, W., 2022. Effect of novel aspergillus and neurospora species-based additive on ensiling parameters and biomethane potential of sugar beet leaves. Appl. Sci. 12, 2684. https://doi.org/10.3390/app12052684.

VDI 4630, 2016. Fermentation of Organic Materials - Characterization of the Substrate, Sampling, Collection of Material Data, Fermentation Tests. Verein Deutscher Ingenieure (VDI), Germany.

Wall, D.M., Straccialini, B., Allen, E., Nolan, P., Herrmann, C., O'Kiely, P., Murphy, J.D., 2015. Investigation of effect of particle size and rumen fluid addition on specific methane yields of high lignocellulose grass silage. Bioresour. Technol. 192, 266–271. https://doi.org/10.1016/j.biortech.2015.05.078.

Warade, H., Mukwane, S., Ansari, K., Agrawal, D., Asaithambi, P., Eyvaz, M., Yusuf, Mohammad, 2025. Enhancing biogas generation: a comprehensive analysis of pre-treatment strategies for napier grass in anaerobic digestion. Discov. Mater. 5, 53. https://doi.org/10.1007/s43939-025-00211-z.

Weber, B., Cruz-Maya, A., Durán-García, Ma.D., Fröhlich, C., 2026. Advanced assessment methods for predicting the biochemical methane potential. Fuel 405, 136496. https://doi.org/10.1016/j.fuel.2025.136496.

Yasim, N.S.E.M., Buyong, F., 2023. Comparative of experimental and theoretical biochemical methane potential generated by municipal solid waste. Environ. Adv. 11, 100345. https://doi.org/10.1016/j.envadv.2023.100345.